Optimization of ^{13}C enrichment by carbon monoxide cryogenic distillation

Laura A. Pellegrini[a*], *Vito A. Sangiorgio*[a], *Giorgia De Guido*[a], *József-Zsolt Szücs-Balazs*[b] *and Mihai Liviu Gligan*[b]

[a]Dipartimento di Chimica, Materiali e Ingegneria Chimica "G. Natta", Politecnico di Milano, Piazza Leonardo da Vinci 32, 20133 Milan, Italy

[b]National Institute for Research and Development of Isotopic and Molecular Technologies (INCDTIM), Donath Street 67-103, 400293 Cluj-Napoca, Romania

**Corresponding author*

Laura A. Pellegrini, e-mail address: laura.pellegrini@polimi.it; full postal address: Dipartimento di Chimica, Materiali e Ingegneria Chimica "G. Natta", Politecnico di Milano, Piazza Leonardo da Vinci 32, 20133 Milan, Italy

ABSTRACT

The main purpose of this study is the optimization of the operating mode for cryogenic distillation columns that provide an isotopic enrichment in stable heavy isotopes. The analysis is based on an experimental cycle for ^{13}C enrichment by CO cryogenic distillation conducted in semi-batch mode in the column of the National Institute for Research and Development of Isotopic and Molecular Technologies. The experimental run is reproduced closely using the simulation software ProSim-BatchColumn, applied for the first time to this type of separations. It is, then, used to investigate the dynamics of the process and the effect of the feed flowrate on the separation to be achieved. As a result, an optimized cycle is proposed, which allows reaching the desired specifications in around one-third the time. The obtained results are interesting and can be applied to all the mixtures where heavy components have a higher commercial value than the light ones.

KEYWORDS

Cryogenic distillation; isotopic enrichment; semi-batch operation; carbon monoxide; optimization.

1. INTRODUCTION

Stable isotopes are non-radioactive variants of a given element. Their different number of neutrons confer them unique properties with several applications in different fields, including water and soil management, environmental studies (Steier et al., 2010), nutrition assessment studies (Owino et al., 2017) and forensics (Aggarwal et al., 2008). Unfortunately, their application is often limited by their high cost of production (Smirnov et al., 2015). During the last decades the usage of stable isotopes has sharply increased in new fields of application as nuclear medicine (Gould, 2009), NMR and PET (Andreev et al., 2007) and this has contributed to raise the interest in the study of separation systems capable of producing larger amounts of ^{18}O, ^{15}N, ^{13}C and other isotopic species, since their market is expected to explode in the next years, as forecasted by Khoroshilov (2018).

Isotopes can be separated through thermal diffusion (Rutherford, 1975), laser separation (Averbukh et al., 1996), centrifugation either single-stage or in cascades (Borisevich et al, 2017) and plasma centrifugation (Borisevich et al., 2019), distillation or other techniques (e.g., membrane distillation for the separation of oxygen-18 water, investigated by Ahadi et al., 2018) that take advantage of the difference in a single physical property. In addition to that, also adsorption-based chromatography has been investigated and proposed for this type of separation. An application for this latter method is given by the recovery of ^{85}Kr from nuclear off-gas: Chen et al. (2013) developed a pressure-swing adsorption (PSA) process for this purpose. For the separation of light elements, the most applied method is distillation (Andreev et al., 2007) (cryogenic for gases that liquefy at very low temperatures), which takes advantage of the difference in vapor pressure of the isotopes to be separated.

The distinctive feature about isotopic mixtures is the great similarity that exists in the components' properties: this makes their separation factor very close to unity and the separation itself quite challenging, though still possible, and different from usual industrial distillation units, such as those used in oil refineries (Ibrahim et al., 2018) and in natural gas processing (De Guido et al., 2018). As reported by McInteer (1980), the implication of this is that plants to separate isotopes are different in their design and construction than those for other separations.

The isotope of interest in this paper is ^{13}C, one of the stable isotopes dominating the market thanks to its successful use in diagnostic and research fields (*e.g.*, archeology), as well as for other purposes, such as breath tests in medical research, which is considered to be a major driver for its market growth (Andreev et al., 2007). As reported by Li et al. (2010), there are several methods to produce the stable isotope ^{13}C, among which cryogenic distillation is the only economic method for industrial production. However, the situation of high cost and low productivity for ^{13}C restricts its large-scale application (Li et al., 2010). Therefore, how to reduce the production cost and to enlarge the production scale has become the biggest problem engineers have faced for a long time. In this work, we propose an operating mode that allows reducing the process time, therefore increasing the productivity.

Enrichment of carbon sources in ^{13}C can be performed through the distillation of isotopic mixtures of a molecular species that contains at least one carbon atom, choosing the one with the highest possible relative volatility between its light and heavy isotopic forms.

From a comparison among some species containing carbon atoms (Table 1), it results that the highest relative volatility, α, (Kister, 1992) occurs for carbon monoxide (CO), which is the ideal candidate to set up a distillation process.

Table 1. Relative volatility of carbon monoxide (Ancona et al., 1962), methane (Johns, 1958), benzene and methanol (Baertschi et al., 1953) containing an atom of ^{13}C.

operating substance	carbon monoxide	methane	benzene	methanol
molecules	$^{12}C^{16}O/^{13}C^{16}O$	$^{12}CH_4/^{13}CH_4$	$^{12}C_6H_6/^{12}C_5{}^{13}CH_6$	$^{12}CH_3OH/^{13}CH_3OH$
$\boldsymbol{\alpha}$	1.00700 @ 81.1 K	1.00300 @ 111.7 K	1.00025 @ 307.4 K	1.00020 @ 307.4 K

The state-of-the-art plants for ^{13}CO production are based on multistage distillation with parallel columns operating in continuous, as the one designed by the Russian Kurchatov Institute Science Centre (Andreev et al., 2007). It is divided in three sections operating in continuous, with a height of 39 m and a diameter equal to 72 mm, filled with random packing. Previously, the design issues of the Los Alamos National Laboratory plant for ^{13}CO production were discussed by McInteer and coworkers (McInteer, 1980; Matwiyoff et al., 1983). More recently, the separation of the isotope ^{13}CO using a high-performance structured packing has been treated by Li et al. (2010), being the height equivalent to a theoretical plate (HETP) a very critical issue for stable isotopes distillation because of their very narrow boiling point range. The control system of a separation column for ^{13}CO enrichment by cryogenic distillation of CO has been studied by Dulf et al. (2009) and Ionescu et al. (2015), while Dumitrache et al. (2012) have proposed three PDE models for the simulation of a CO cryogenic distillation process for ^{13}C isotope separation.

This paper deals with the simulation of CO cryogenic distillation for enrichment in ^{13}CO with the aim of: *i)* evaluating and optimizing the performances of the semi-batch operating mode, and *ii)* building up a useful model that may be exploited for small discontinuous productions. To pursue these goals, established methods well known in the field of chemical and process engineering have been used and a commercially available software (ProSim-BatchColumn) has been employed both for process simulation (described in section 3) and design, after validation against experimental data from a pilot distillation column (presented in section 2). Once the model reliability has been proved (as shown in section 4.1), an optimized operating procedure is proposed in section 4.2.

2. EXPERIMENTAL

This section deals with the detailed description of the pilot distillation column that has provided the experimental data used to assess the reliability of the simulation results. In addition to that, also its operating mode is described, since the considered operation is different from the conventional batch or continuous distillations that are commonly found in process engineering.

The experimental plant (Figure 1) consists of a random packing distillation column filled with Heli-Pack 2x2x0.2 mm stainless steel, having an internal diameter (*ID*) equal to 26 mm and a height (*Z*) equal to 7.032 m, with the feed point located 2500 mm under the top, as described by Radoi et al. (1999). The ratio *Z*/*ID* is significantly higher than the one found in heuristics for distillation columns (Branan, 1994), which is due to the very high number of theoretical stages required and, at the same time, to the small flowrates of isotopic distillation in comparison with non-isotopic ones. A vacuum jacket, where the pressure is maintained at $2 \cdot 10^{-5}$ mmHg, reduces heat losses due to irradiation (Tien and Cunnington, 1973). The feeding system works at atmospheric pressure and the operating pressure inside the column is around 0.85 bar, due to pressure drops in the upstream pieces of the equipment. The temperature is about 80 K, which is the boiling point of pure CO at the operating pressure. The reboiler in the bottom is electric and it provides an adjustable duty in the order of 100 W, while the condenser removes a comparable amount of thermal power using liquid nitrogen.

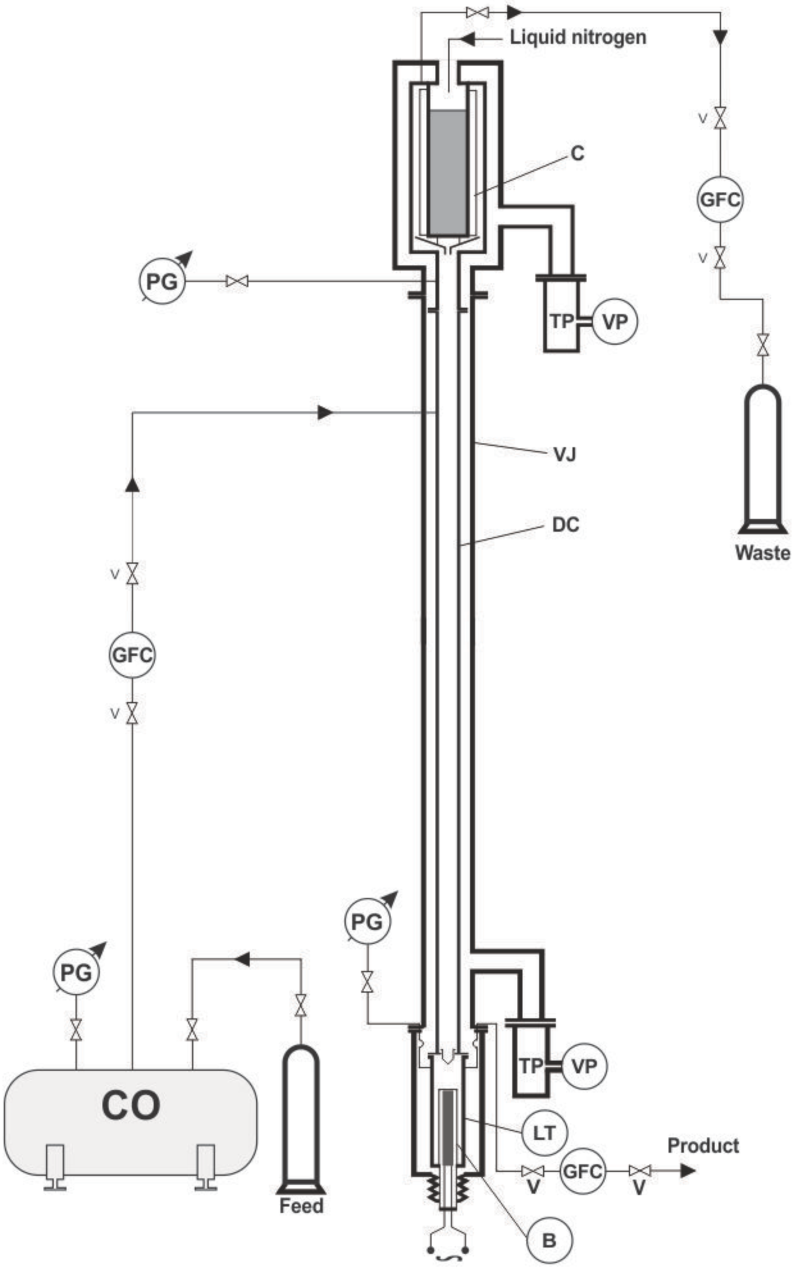

Figure 1. Experimental plant for ^{13}CO enrichment: *B* - boiler, *C* - condenser, *DC* - distillation column, *GFC* - gas flow controller, *LT* - level transducer, *PG* - pressure gauge, *TP* - turbomolecular pump, *V* - valve , *VJ* - vacuum jacket, *VP* - vacuum pump.

The experimental run lasted 451 hours and is divided into 3 different phases as follows: 200 h at total reflux, 232 h in semi-batch mode, the last 19 h at total reflux. The feed mixture consists of highly *in-situ* purified CO. The molar mass initially fed into the column for total reflux operation is estimated to be around 13 mol. In the semi-batch mode, the CO stream (0.19/0.12 mol/h) is continuously fed into the column and a distillate product is produced at the top, while no product is withdrawn from the bottom.

Experimental data are reported in Table 2. x_T and x_B represent the molar fraction of ^{13}CO measured through samplings, respectively, at the top and in the bottom of the column.

Table 2. Experimental data for ^{13}CO enrichment by carbon monoxide cryogenic distillation in total reflux and semi-batch operating modes.

Time [h]	ΔP [mbar]	Hold-up boiler [mol]	Feed [mol/h]	x_T [mol %]	x_B [mol %]	Boiler power [W]
8	100	0.24	0	1.064	1.668	100
19	130	0.46	0	0.431	2.080	100
21.5	120	0.57	0	0.393	2.034	100
31.5	115	0.58	0	0.313	2.132	100
45	115	0.61	0	0.308	2.244	100
57	115	0.62	0	0.318	2.170	100
69	115	0.70	0	0.349	2.227	100
81	115	0.62	0	0.306	2.244	100
93	115	0.67	0	0.359	2.178	100
118.5	120	0.76	0	0.318	2.200	100
141.5	120	0.76	0	0.327	2.227	100
165.5	110	0.60	0	0.372	2.162	100
189	110	0.68	0	0.323	2.218	100
201	125	0.90	0.19	0.311	2.194	105
212.5	130	1.57	0.19	0.367	2.185	105
224.5	145	0.61	0.19	0.414	2.482	105
236.5	130	0.45	0.19	0.436	2.635	105
248.5	140	0.43	0.19	0.441	2.929	105
260.5	140	0.51	0.19	0.494	3.194	105
272.5	140	0.46	0.19	0.501	3.364	105
282.5	140	0.23	0.19	0.557	3.624	105
294.5	135	0.35	0.19	0.577	3.853	105
306.5	135	0.45	0.19	0.578	3.916	105
318	140	0.36	0.19	0.603	4.175	105
330	135	0.21	0.19	0.627	4.327	105
342	135	0.32	0.19	0.644	4.314	105
354	135	0.25	0.19	0.627	4.702	105
366	135	0.37	0.19	0.645	4.818	105
390	140	0.38	0.12	0.665	4.877	105
414	135	0.44	0.12	0.692	4.966	105
432	135	0.20	0.12	0.694	5.161	105
451	135	0.32	0	0.625	5.535	105

3. SIMULATION

In the following, the bases of the analysis are explained, focusing on the modelling of the system under investigation and on the set-up of the process simulator.

Setting up a suitable model for the separation of the isotopic mixture inside the column is a key element on which the whole simulation reliability is based. Since the stream of carbon monoxide presents a high degree of purity, CO is assumed to be the only chemical species inside the mixture. In these conditions, it is possible to appreciate the separation of different CO isotopes inside the column. It is useful to recall that, according to de Laeter et al. (2003), C has two naturally occurring stable isotopes (^{12}C=98.83%, ^{13}C=1.07%) and O has three stable isotopes (^{16}O=99.757%, ^{17}O=0.038%, ^{18}O=0.205%). For this reason, in every CO stream it is possible to find 6 different isotopic combinations, of which $^{13}C^{17}O$ and $^{13}C^{18}O$ can be neglected, due to their very low concentration. As for the isotopes $^{12}C^{17}O$ and $^{12}C^{18}O$, their concentration is five times lower than the one of $^{13}C^{16}O$, which is the species of interest, and their vapour pressure is closer to that of $^{12}C^{16}O$: they, therefore, distribute along the column without a significant accumulation in the reboiler. It can also be pointed out that the final enrichment in the experimental run is limited to around 5 mol % in ^{13}CO (Table 2): in case significantly higher enrichments are required, also heavy oxygen isotopes should be taken into account. Therefore, it is reasonable to simplify the feed stream to a binary mixture of $^{13}C^{16}O$ (heavy key) and $^{12}C^{16}O$ (light key) and apply the strategies normally used to solve binary distillation. The relative volatility is considered constant and equal to α=1.007 (Johns, 1958), since no significant pressure drops were measured between top and bottom of the column and temperature differences were estimated to be not relevant.

For the simulation of the process under investigation, the simulation software ProSim-BatchColumn (ProSim, 2017) has been selected, specifying the Antoine equation as thermodynamic model, since it allows to manage batch, semi-batch and continuous distillations in the same simulation. The flexibility of this software comes from the possibility of assigning different operating conditions at established intervals through the construction of a detailed scenario during time. In addition, the properties of streams interacting with the column are independent of upstream and downstream units, so that it is possible to evaluate column performances not affected by dynamics and disturbances of other operating units.

A number of input data are required to fully characterise the system, including temperature, pressure, number of theoretical stages (*N*), initial load, liquid hold-up in the reboiler, inlet mole fraction of ^{13}CO, duty. As for the condenser, the duty is assumed to be almost equal to the reboiler one and the hold-up is smaller than 0.1 mol, which represents few droplets stuck on the cold surface. Once the input data are assigned, a detailed scenario describing the experiment schedule in terms of power, inlet flowrate, distillate flowrate has been defined coherently with the experimental conditions and implemented into the simulation software. It is important to highlight that the model validation and the consequent optimization are carried out benefitting by the numerical solution of an extent system of equations built-in into ProSim-BatchColumn. This time-dependent system includes mass balances, energy balances, equilibrium equations for each equilibrium stage. This tool allows the detailed evaluation of system’s dynamics, which would not be possible through classical shortcut methods applied to distillation columns.

3.1. OPERATION AT TOTAL REFLUX

The main datum to be provided by the user, which is not directly measurable, is the number of theoretical stages equivalent to the height of the packed section. It can be estimated using the Fenske equation, which, in terms of the molar fractions of the less volatile compound ^{13}C^{16}O, takes the form of Eq. (1).

$$\alpha^{N} = \frac{\dfrac{x_B}{(1-x_B)}}{\dfrac{x_T}{(1-x_T)}} \qquad (1)$$

It is well known that the Fenske formula fits well total reflux operation (Gualito et al., 1997) and, consequently, its range of applicability is limited to the first 189 hours of the experimental campaign. However, in the first part of the experiment the column cannot be considered at steady state yet due to an unstable fluid dynamic behaviour. For this reason, the first four measures reported in Table 2 have been neglected in the following estimation. The number of theoretical stages (*N*) has been found applying Eq. (1) to the experimental results comprised between 45 h and 189 h and, then, calculating the average of the resulting values, which is equal to *N*=275±13, as represented in Figure 2. The confidence interval of the average *N* is calculated applying a t-test with a confidence level of 99% and in percentage terms it is equal to N=275±4.6%. The confidence interval is narrow enough to assume *N*=275 as an input datum to be introduced into the simulation software.

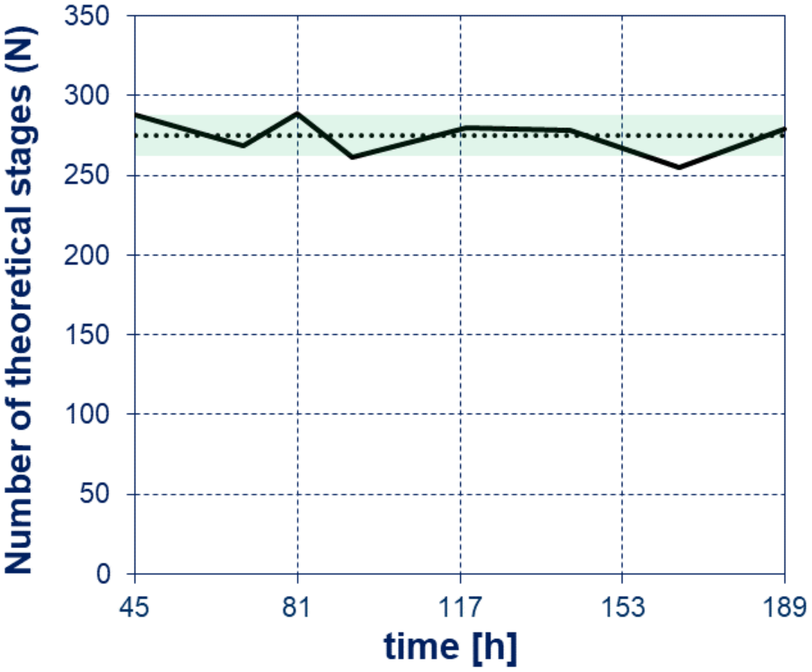

Figure 2. Number of theoretical stages calculated by applying Eq. (1) to the experimental data reported in Table 2 for t = 45-189 h (solid line). The dotted line represents the average number of theoretical stages. The confidence interval calculated applying a t-test with a confidence level of 99% is shown in light blue.

Concerning the liquid hold-up in the reboiler (*H*), it can be approximated to a constant value during the total reflux operation in the first part of the experimental campaign. This approximation comes from the observation of randomly distributed measures, without any evident trend found from the experimental data during the steady state phase ranging between 45 h and 189 h. The liquid hold-up has been estimated to be H=0.67±0.07 mol calculated applying a t-test with a confidence level of 99%, that in percentage terms is equal to H=0.67±10.3% mol. Therefore, the initial hold-up, which has to be introduced as an input parameter into the simulation software, is assigned equal to 0.67 mol and it is kept constant in the first phase of the simulation, up to 200 h. Moreover, it has to be noted that oscillations in the order of 0.07 mol in the liquid hold-up are significantly lower than the total liquid hold-up contained in the whole column including the packing, which is around 13 mol during the start-up phase.

3.2. SEMI-BATCH OPERATING MODE

In order to model the system during the semi-batch operation, the total material balance on the whole column can be represented by Eq. (2), considering the moles of liquid hold-up on each equivalent tray (S_i, where i refers to the generic i-th equivalent tray) to be constant. In Eq. (2), H denotes the bottom hold-up [mol], t the time [h], F the feed flowrate [mol/h], D and B the distillate and bottom flowrates [mol/h], respectively.

$$\frac{dH}{dt} = F - D - B \qquad (2)$$

The assumption of a constant S_i is reasonable referring both to time-weighted average and spatial-weighted average values, since temperature, pressure, internal liquid and vapor flowrates remain almost constant during the whole process and over the whole length of the distillation column. Therefore, it is possible to assume that the fluid dynamic behavior of the column is on average constant and homogeneous.

During the semi-batch operation phase, it is necessary to assign both the feed flowrate (*F*) and the distillate flowrate (*D*), whereas the bottom flow rate (*B*) is null. According to Eq. (2), *D* can be computed as the sum of the feed flowrate and a smaller contribution given by the evaporation of the liquid hold-up in the reboiler, due to a slightly decreasing trend observable on the boiler hold-up values in Table 2, between 201 h and 432 h. It is important to highlight that this second term is far smaller than the contribution given by the inlet flowrate and it could be evaluated by simple analysis of the quantities at stake, introducing the evaporation rate of the liquid hold-up, $\frac{\Delta \mathrm{H}}{\Delta \mathrm{t}}$, which is useful for this purpose. This term is calculated as the difference between the liquid hold-up at steady state, H(@ t=200 h) = 0.67 mol, and the experimental value at the end of the semi-batch distillation phase, H(@ t=432 h) = 0.20 mol, divided by the difference between the respective time values. The evaporation rate of the liquid hold-up in the reboiler is found to be $\frac{\Delta \mathrm{H}}{\Delta \mathrm{t}} \sim 0.002\ \mathrm{mol/h}$. To obtain the distillate flowrate (*D*), this quantity has to be summed to the feed flowrate (*F*) which is first equal to *F*=0.19 mol/h and is, then, decreased to *F*=0.12 mol/h. In Table 3, the calculated values of *D* are reported next to the respective *F*.

Table 3. Calculated values of the distillate flowrate (*D*) associated to the respective feed flowrate (*F*) during the experimental semi-batch operating mode.

Time range [h]	**F [mol/h]**	$\frac{\Delta H}{\Delta t}$ **[mol/h]**	**D [mol/h]**	**F :** $\frac{\Delta H}{\Delta t}$ **ratio**
201→366	0.19	0.002	0.192	95:1
366→432	0.12	0.002	0.122	60:1

Among the results obtained by this analysis, there is an interesting point that is worth being pointed out: the contribution given by F to the distillate flowrate is several times higher than the contribution given by the evaporation of the liquid hold-up into the reboiler, as shown in the last column of Table 3. It follows that the main reason causing the enrichment into the column is given by the semi-batch operation and not by the classic evaporation of a conventional batch operating mode, which gives a very small contribution. However, this minor phenomenon has been included into the simulation to guarantee the coherency with the experiment.

In order to enhance the understanding of the phenomenon occurring into the distillation column, it is useful to show the profiles of the ^{13}CO molar fraction along the column (x_i, where i refers to different column heights in the range 0-7 m), that are reported in Figure 3. These profiles are reconstructed from the experimental data reported in Table 2, assuming a constant relative volatility along the column and setting as reference values the experimental molar fractions, x_B in the bottom and x_T at the top. The two profiles shown in Figure 3 are referred to time instants where the column is operated at total reflux. In particular, at 189 h the steady state is achieved before any feed being introduced into the column, while at 451 h the steady state is achieved to let the column equilibrate after the end of the distillation process. The vertical dashed line is drawn at a fixed value of x_i=1.07 mol%, corresponding to the natural abundance of ^{13}CO and, therefore, to the molar fraction of the feed being introduced during the semi-batch operating mode. This line has to be taken as a reference to understand that after 189 h, at steady state, a redistribution of the heavy isotope is observed along the distillation column, increasing the molar fraction of the heavy isotope in the bottom. Moreover, looking at the intersections between the two curves and the vertical line, it is possible to note that the profile of x_i has been shifted rightwards after the distillation process and that the height at which x_i=1.07% is found has been shifted upwards, highlighting an overall enrichment of the liquid phase in ^{13}CO into the distillation column. From this observation, it becomes more evident that feed supply acts a major role in the enrichment process during the semi-batch operating mode.

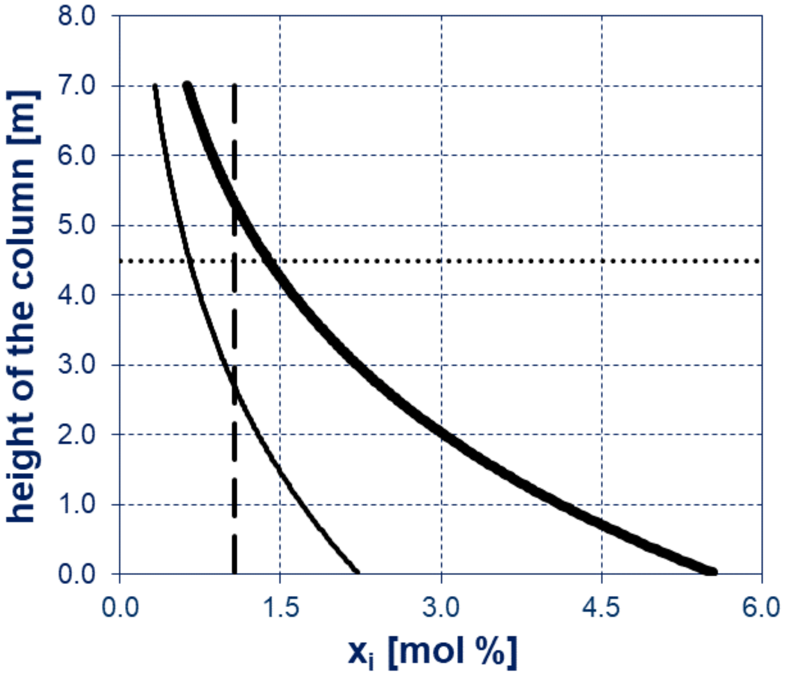

Figure 3. Reconstructed profiles of ^{13}CO molar fraction along the column (*x*$_i$, where *i* refers to different column heights in the range 0-7 m) at two different time instants when the cryogenic distillation column is operated at total reflux (— t=189 h; ▬ t=451 h). The natural abundance of ^{13}CO=1.07 mol% (dashed vertical line) and the feed inlet point at a height of 4.5 m (dotted horizontal line) are also shown.

4. RESULTS

In this section, the results of the simulation of the experimental campaign are first presented, for a model validation. Then, the optimization procedure is proposed, which has been defined using the simulator to optimize the operation of the column by minimizing the operation time.

4.1. MODEL VALIDATION

As a first step, the model implemented in ProSim-BatchColumn (ProSim, 2017) was validated by simulating the experimental run and evaluating the deviation of the model results from the experimental data.

Simulation outputs in terms of molar fractions x_T and x_B are reported in Figure 4, where the trends, including start-up, steady state at total reflux and enrichment phase (semi-batch operation) show a good agreement with experimental data, as also proved by comparing in Table 4 some significant figures from the experimental run and from the simulation.

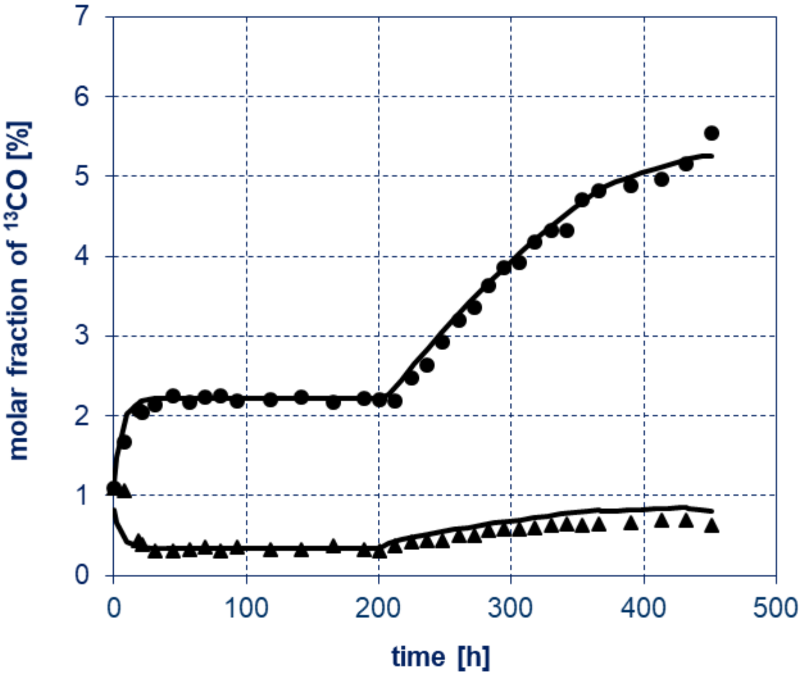

Figure 4. ^{13}CO molar fractions at the top (x_T) and in the bottom (x_B) of the distillation column (shown in Figure 1) from simulation (continuous lines) and from the experimental run (●: x_B; ▲: x_T).

The steady state is well approximated both for x_B and x_T, since the output values of the simulator correspond to the experimental average values, which are respectively 2.21 mol %

and 0.33 mol %. These results, shown in Figure 4, confirm that the approximations introduced into the model are reasonable and that the number of theoretical stages is well estimated by the Fenske equation (Eq. (1)).

Table 4. Comparison of simulated and experimental molar fractions x_T and x_B with relative errors.

Time [h]	**Simulated x_B [mol %]**	**Experimental x_B [mol %]**	**Relative error on x_B**	**Simulated x_T [mol %]**	**Experimental x_T [mol %]**	**Relative error on x_T**
200	2.21	2.20	0.005	0.33	0.33	0
366	4.83	4.85	0.004	0.82	0.69	0.188
432	5.20	5.16	0.008	0.85	0.70	0.214
451	5.26	5.53	0.049	0.81	0.62	0.306

As for the enrichment phase, *i.e.* the semi-batch operation, a separate discussion has to be made for x_B and x_T. The simulated curve of x_B in Figure 4 is in very good agreement with the experimental data and this accuracy proves the model reliability in representing the enrichment of ^{13}CO, which concentrates in the bottom. The only point that differs between the simulation and the experiment is the last measure after a re-equilibrium phase at total reflux: it is not easily understandable if that measure is simply affected by error or if, in the real column, this step causes a greater separation than the one predicted through the simulation. The simulated curve of x_T has the same trend of the experimental points in the enrichment section, but the numerical values differ on average by around 0.15 mol %, which is low but not negligible. However, this is not seen as an issue that may affect the optimization as long as the stream out-going from the top of the distillation column is considered a waste and the valuable product is in the bottom. In conclusion, the simulation of the experiment can be considered successful and it lays the foundations for the optimization procedure described in the following.

4.2 PROPOSED OPTIMIZED PROCEDURE

Several variables can be considered for the system optimization. It is important to distinguish between easily achievable modifications and the ones that require structural modifications of the plant, which are not considered at all. As an example, the feed temperature belongs to the second class since, to modify it, a heat exchanger has to be introduced from scratch. Among the variables that can be moved during the semi-batch phase, the only one that causes appreciable differences in the column performances is the feed flowrate (F). Understanding how the system behaves at different F values is the key point of the whole optimization: low values of F lead to high x_B asymptotical values after long times, while high values of F lead to lower x_B asymptotical values, but in significantly shorter times. This behaviour is shown in Figure 5, where simulation results are reported for F equal to 0.19 mol/h (as in the run of the pilot column) and for F equal to 0.40 mol/h and 0.70 mol/h.

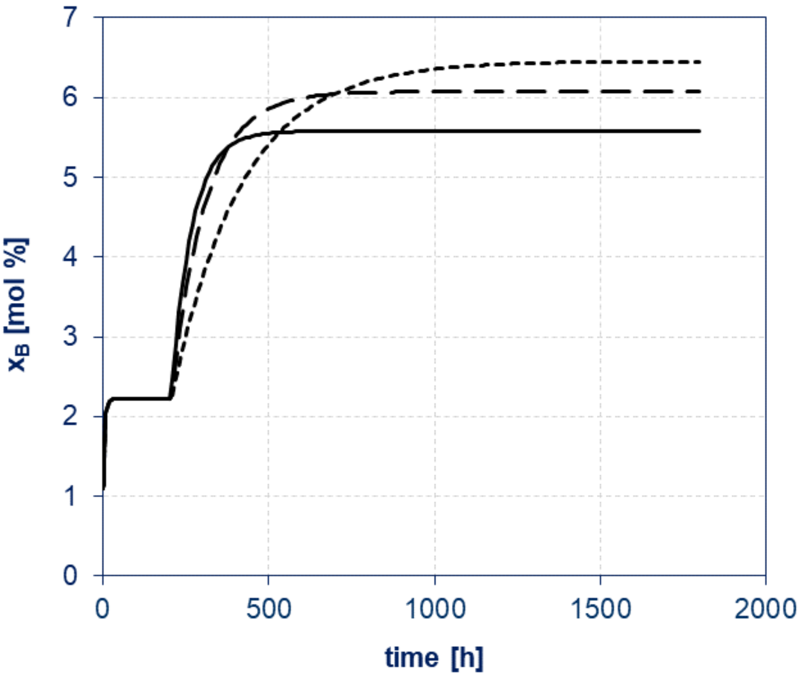

Figure 5. Simulated trend of the molar fraction x_B during time in ^{13}CO enrichment by carbon monoxide cryogenic distillation in total reflux and semi-batch operating modes for different feed flowrates (- - - - F=0.19 mol/h; – – – F=0.40 mol/h; — F=0.70 mol/h).

The idea in the choice of *F* is to always use the value that ensures the highest derivative dx_B/dt, that can be seen as a rate of enrichment; it follows that, at the beginning, higher values of *F* need to be set, while, at the end, lower *F* values can be chosen. The highest value of *F* is not higher than 1.0 mol/h to prevent significant alterations of the original fluid dynamic behavior of the column, since *F* enters the cryogenic column at room temperature, and this causes an extra evaporation of the liquid stream flowing inside the column and, consequently, a higher vapor flowrate. The feed flowrate follows a monotonic decreasing path during time: the function $F_{opt}=f(x_B)$ can be obtained numerically through finite differences evaluation where, for each couple of adjacent feed values, the optimum switching point in terms of x_B (the highest derivative dx_B/dt) is determined. A graph of the optimum *F* is illustrated in Figure 6.

The dependence of column dynamics on the value of the feed flowrate (F) is the key of the optimization presented in this paper. It is necessary to highlight that F_{opt} is defined as $F_{opt}=f(x_B)$ to drop the dependence on time, since in this way it becomes independent of the operating conditions before the semi-batch phase starts. However, if a detailed economic evaluation is required, it is useful to have it as $F_{opt}=f(t)$ to choose the first and the last F and to set an acceptable bias for $F(t)$ to be adopted.

Since on the pilot column flow regulation is not automated and continuous regulation is not allowed, a discontinuous line drawn with only three decreasing values of F (*i.e.*, 1.0, 0.70, 0.40 mol/h) has been considered (Figure 6). For the economic assessment of the distillation process, it is necessary to point out that paths above the “optimum line” in Figure 6 are not economically advantageous, since a higher waste (*i.e.*, distillate flowrate at the top of the column) is produced and lower performances are achieved. Paths below the “optimum line” are economically advantageous since they produce lower waste, but their performances are lower. In the region comprised between the optimum feed line and the value (0.19/0.12 mol/h), used in the experimental run, it is possible to find the best compromise between costs and performances. The “proposed line”, which considers only three decreasing flowrates, falls in this region.

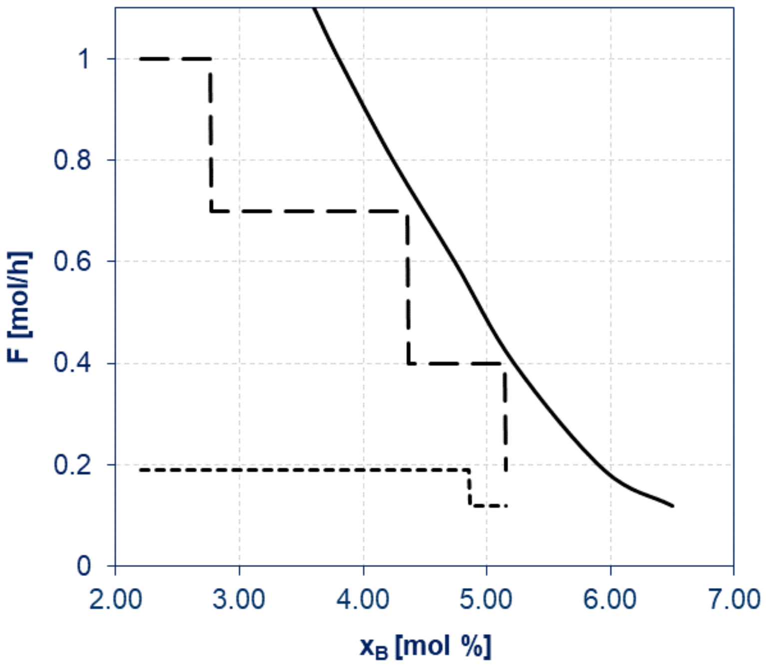

Figure 6. Feed flowrate *vs.* ^{13}CO molar fraction x_B in ^{13}CO enrichment separation by carbon monoxide cryogenic distillation in the semi-batch operating mode: optimum line (—), proposed line (– – –) and experimental line (- - - -).

At this point, an improved cycle based on the "proposed line", called "short cycle" in the rest of the paper, can be analyzed. Values of the reboiler duty are chosen on the basis of the simulation described in section 4.1, in order to maintain comparable flows inside the column and not to exceed the recommended flooding limits.

After feed flowrate modification, the simulation was run and it was found that the "short cycle" ends 109 hours before the "experimental cycle", corresponding to the original simulation of the experimental run. The simulation was stopped when x_B reached the target value of 5.26 mol %, as in the previous simulation. Graphically, it results in a curve of x_B with a greater slope, (continuous line in Figure 7), which corresponds to the criterion chosen for the optimization.

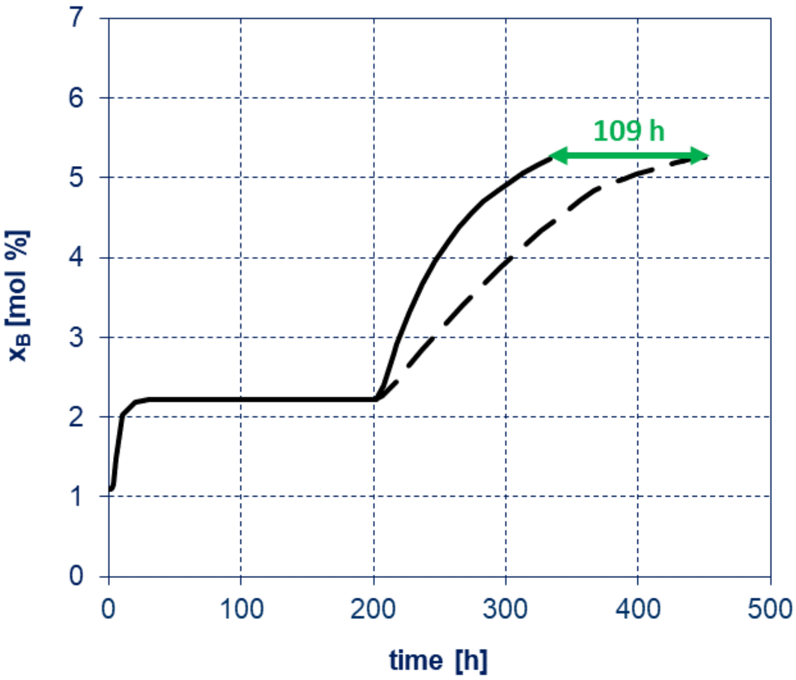

Figure 7. Simulated molar fraction x_B *vs.* time in the "short cycle" (—) compared with the experimental cycle (– – –) for ^{13}CO enrichment by carbon monoxide cryogenic distillation in total reflux and semi-batch operating modes.

Another improvement on the cycle can be made focusing on the steady state section (total reflux), due to the fact that in the experimental run it is overextended. This results in a long period that is unexploited for isotopic enrichment, since the slope of a steady state phase is null. The key consideration is that it is not necessary to reach steady state conditions for x_B, but it is useful to operate at total reflux at the beginning because this phase has a high slope in the first 10 hours and it does not produce any waste. On the other hand, the total reflux phase is necessary to achieve fluid dynamic stability inside the column and, in case it takes more than 10 hours to reach steady state conditions, it is recommended to start in semi-batch mode as soon as settled. Passing, for the total reflux phase, from 200 hours to 10 hours allows reducing the operation time by 190 extra hours, which, together with the 109 hours saved thanks to feed optimization, leads to a total saving with the "short cycle" of 299 hours (Figure 8). Scheduling of "short cycle" in its final shape is reported in Table 5.

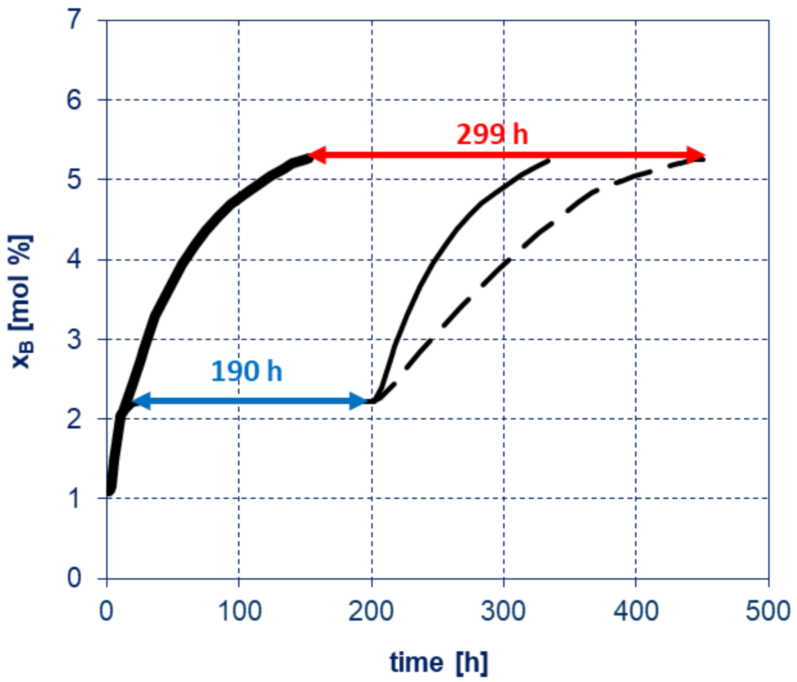

Figure 8. Simulated molar fraction *x_B* vs. time in the “short cycle” with 10 hours (▬) and 200 hours (—) of total reflux operation compared with the experimental cycle (– – –) for ^{13}CO enrichment by carbon monoxide cryogenic distillation in total reflux and semi-batch operating modes.

Table 5. Scheduling of the “short cycle” compared with the “experimental cycle”.

Phase	**Experimental cycle**	**Short cycle**
total time [h]	451	152
total reflux [h]	200	10
semi-batch (*F*=1.0 mol/h) [h]	–	15
semi-batch (*F*=0.70 mol/h) [h]	–	50
semi-batch (*F*=0.40 mol/h) [h]	–	58
semi-batch (*F*=0.19 mol/h) [h]	166	–
semi-batch (*F*=0.12 mol/h) [h]	66	–
riequilibrium [h]	19	19

The comparison of the “short cycle” with the “experimental cycle” shows that the former one lasts 152 hours instead of 451 hours, which is almost one third of the original time: this means that every time the column has to be started-up for $^{13}C^{16}O$ production, the cycle will be more than 12 days shortened. Large time reduction leads to interesting cost savings related to reduced liquid nitrogen consumption at the condenser, reduced human labour and reduced expenses for external utilities. The only drawback about the “short cycle” is that the total waste is increased in comparison with the “experimental cycle” (73 mol instead of 40 mol of CO after the whole cycle), as a direct consequence of higher F and, consequently, D flowrates. However, the total waste is less than doubled and, since in isotopic distillation columns feed and waste have the same chemical purity, they have the same economic value for a chemical customer that is not interested in isotopic abundance. For this reason, higher waste may not necessarily be seen as a disadvantage mainly if coupled to a significant operation time reduction.

5. CONCLUSIONS

In this paper, the cryogenic distillation of carbon monoxide is discussed in order to obtain an isotopic enrichment in ^{13}CO, considering the importance it assumes due to its successful use in diagnostic and other research fields The experimental run of a distillation pilot column placed at the National Institute for Research and Development of Isotopic and Molecular Technologies Cluj-Napoca (INCDTIM), consisting of a total reflux phase followed by a semi-batch one, has been considered for performing its simulation and optimization. First, a simulation model of the distillation system has been built up: the good agreement between the experimental data and the simulation results proved the reliability of the model. As a second step, those variables that can be easily modified and their impact on column performances have been analysed. The most interesting dependence has been found between the feed flowrate and ^{13}CO enrichment velocity in the bottom of the column. A general trend valid for the semi-batch operating mode has been found, and a function of the optimum feed flowrate has been built to achieve a faster operation. Exploiting this concept, it has been possible to develop an improved cycle tailored for the INCDTIM column and to provide a schedule for column's future optimized runs. The proposed cycle is significantly shorter than the experimental one, reducing the required time to one-third without affecting the final conditions inside the column. This strategy makes evident that software-supported optimization is a powerful method to optimize distillation column operation during time-depending runs without the need for too expensive experimental campaigns. This tool becomes important in systems where high costs or long times are required for experiments, as in the case of isotopic distillation of CO, Ar, N_2, NO, H_2O, NH_3 heavy stable isotopes, allowing significant improvements otherwise unaffordable.

ABBREVIATIONS

HETP	height equivalent to a theoretical plate
INCDTIM	National Institute for Research and Development of Isotopic and Molecular Technologies Cluj-Napoca
NMR	Nuclear magnetic resonance
PET	Positron emission tomography
PDE	Partial differential equation
PSA	Pressure-swing-adsorption

SYMBOLS

B	bottom flowrate [mol/h]
^{12}C	carbon atom with mass number 12
^{13}C	carbon atom with mass number 13
D	distillate flowrate [mol/h]
F	feed flowrate [mol/h]
F_{opt}	optimum feed flowrate [mol/h]
H	bottom hold-up [mol]
ID	column internal diameter [mm]
N	number of theoretical stages
^{15}N	nitrogen atom with mass number 15
^{18}O	oxygen atom with mass number 18
S_i	generic equivalent tray hold-up [mol]
t	time [hours]
x_B	molar fraction of ^{13}CO in the bottom of the column
x_i	molar fraction of ^{13}CO on a generic equivalent tray
x_T	molar fraction of ^{13}CO at the top of the column
Z	column height [m]

Greek symbols

α	relative volatility
ΔP	pressure drops [mbar]

REFERENCES

Aggarwal J., Habicht-Mauche, J., Juarez, C., 2008. Application of heavy stable isotopes in forensic isotope geochemistry: A review. *Applied Geochemistry 23*(9), 2658-2666. doi:10.1016/j.apgeochem.2008.05.016.

Ahadi, H., Karimi-Sabet, J., Shariaty-Niassar, M., Matsuura, T., 2018. Experimental and numerical evaluation of membrane distillation module for oxygen-18 separation. *Chemical Engineering Research and Design 132*, 492-504. doi.org/10.1016/j.cherd.2018.01.042.

Ancona, E., Boato, G., Casanova, N., 1962. Vapour pressure of isotopic liquids. *Il Nuovo Cimento* 24, 111-121. doi:10.1007/BF02785764.

Andreev, B.M., Magomedbekov, E.P., Raitman, A.A., Pozenkevich, M.B., Sakharovsky, Y.A., Khoroshilov, A.V., 2007. *Separation of Isotopes of Biogenic Elements in Two-phase Systems*. Moscow: Elsevier.

Averbukh, I.S., Vrakking, M.J.J., Villeneuve, D.M., Stolow, A., 1996. Wave Packet Isotope Separation. *Physical review letters 77*(17), 3518-3521. doi:10.1103/PhysRevLett.77.3518.

Baertschi, P., Kuhn, W., Kuhn, H., 1953. Fractionation of isotopes by distillation of some organic substances. *Nature 171*(4362), 1018-1020.

Borisevich, V.D., Yan, J., Smirnov, A.Y., Bonarev, A.K., Zeng, S., Sulaberidze, G.A., Jiang, D., 2017. Cascade design for isotopically modified molybdenum as an alternative to zirconium alloys. *Chemical Engineering Research and Design 128*, 257-264. doi.org/10.1016/j.cherd.2017.10.018.

Borisevich, V.D., Potanin, E.P., Whichello, J.V., 2019. Isotope separation of low boiling-point substances by plasma centrifuge with circulation. *Separation Science and Technology*, 1-10. doi:10.1080/01496395.2019.1606830.

Branan, C.R., 1994. *Rules of Thumb for Chemical Engineering*. Gulf Publising Company, Texas.

Chen, J., Hsu, S.J., Wei, T.Y., 2013. Optimization design for removal of radioactive Kr from Xe using pressure swing adsorption. *Chemical Engineering Research and Design 91*(4), 649-659. doi.org/10.1016/j.cherd.2013.02.003.

De Guido, G., Fogli, M.R., Pellegrini, L.A., 2018. Effect of heavy hydrocarbons on CO_2 removal from natural gas by low-temperature distillation. *Industrial & Engineering Chemistry Research 57*(21), 7245-7256. doi.org/10.1021/acs.iecr.8b00614.

de Laeter, J.R., Böhlke, J.K., De Bièvre, P., Hidaka, H., Peiser, H.S., Rosman, K.J.R., Taylor, P.D.P., 2003. Atomic weights of the elements. Review 2000 (IUPAC Technical Report). *Pure and applied chemistry 75*(6), 683-800. doi:10.1351/pac200375060683.

Dulf, E.-H., Festila, C., Dulf, F., 2009. Monitoring and Control System of a Separation Column for ^{13}C Enrichment by Cryogenic Distillation of Carbon Monoxide. *International Journal of Mathematical Models and Methods in Applied Sciences 3*(3), 196-203.

Dumitrache, D.C., De Schutter, B., Huesman, A., Dulf, E., 2012. Modeling, analysis, and simulation of a cryogenic distillation process for ^{13}C isotope separation. *Journal of Process Control 22*(4), 798–808. doi:10.1016/j.jprocont.2012.02.010.

Gould, P., 2009. Medical isotope shortage reaches crisis level; robust solutions sought urgently to shore up fragile supply chain. *Nature 460*(7253), 312-314.

Gualito, J.J., Cerino, F.J., Cardenas, J.C., Rocha, J.A., 1997. Design method for distillation columns filled with metallic, ceramic, or plastic structured packings. *Industrial & Engineering Chemistry Research 36*(5), 1747-1757. doi: 10.1021/ie960625z.

Ibrahim, D., Jobson, M., Li, J., Guillén-Gosálbez, G., 2018. Optimization-based design of crude oil distillation units using surrogate column models and a support vector machine. *Chemical Engineering Research and Design 134*, 212-225. doi.org/10.1016/j.cherd.2018.03.006.

Ionescu, C., Both, R., Fustos, C., Festila, C., Gligan, M., Keyser, R.D., 2015. Control of a Train of High Purity Distillation Columns for Efficient Production of ^{13}C Isotopes. In: *2015 20th International Conference on Control Systems and Computer Science (pp. 49-56). IEEE.* doi:10.1109/CSCS.2015.150.

Johns, T.F., 1958. Vapor pressures of some isotopic substances. In: *Proceedings of the International Symposium on Isotope Separation,* Eds. J. Kistemaker, J. Bigeleisen, A.O.C. Hier, North-Holland Publishing Company, Amsterdam, p. 74.

Khoroshilov, A.V., 2018. Production of stable isotopes of light elements: past, present and future. *Journal of Physics: Conference Series 1099*(1), p. 012002. doi:10.1088/1742-6596/1099/1/012002.

Kister, H.Z., Haas, J.R., Hart, D.R., Gill, D.R., 1992. *Distillation design* (Vol. 1). New York: McGraw-Hill.

Li, H.L., Ju, Y.L., Li, L.J., Xu, D.G., 2010. Separation of isotope ^{13}C using high-performance structured packing. *Chemical Engineering and Processing: Process Intensification 49*(3), 255-261. doi:10.1016/j.cep.2010.02.001.

Matwiyoff, N.A., McInteer, B.B., Mills, T.R., 1983. Stable Isotope Production - a distillation process. *Los Alamos Science 65*.

McInteer, B.B., 1980. Isotope separation by distillation: design of a carbon-13 plant. *Separation Science and Technology 15(3),* 491-508. doi:10.1080/01496398008068494.

Owino, V.O., Slater, C., Loechl, C.U., 2017. Using stable isotope techniques in nutrition assessments and tracking of global targets post-2015. *Proceedings of The Nutrition Society 76*(4), 495-503. doi:10.1017/S0029665117000295.

ProSim, 2017. ProSim-BatchColumn. ProSim SA, F-31670 Labège Cedex, France.

Radoi, A., Gligan, M., Dronca, S., Radu, D., Axente, D., 1999. ^{13}C enrichment by cryogenic distillation of carbon monoxide on experimental pilot plant. *Conference on Isotopic and Molecular Processes*, 143. National Institute for Research and Development of Isotopic and Molecular Technologies, Romania.

Rutherford, W.M., 1975. Separation of Isotopes in the Thermal Diffusion Column, *Separation and Purification Methods 4*(2), 305-350, doi:10.1080/03602547508066043.

Smirnov, A.Y., Sulaberidze, G.A., Xie, Q., Borisevich, V.D., 2015. Design of cascade with locally enlarged flow for enrichment of intermediate components of multi-isotope mixtures. *Chemical Engineering Research and Design 95*, 47-54. doi.org/10.1016/j.cherd.2014.12.012.

Steier, P., Dellinger, F., Forstner, O., Golser, R., Knie, K., Kutschera, W., Priller, A., Quinto, F., Srncik, M., Terrasi, F., Vockenhuber, C., Wallner, A., Wallner, G., Wild, E.M., 2010. Analysis and application of heavy isotopes in the environment. *Nuclear Instruments and Methods in Physics Research Section B: Beam Interactions with Materials and Atoms 268*(7-8), 1045-1049. doi:10.1016/j.nimb.2009.10.094.

Tien, C.L., Cunnington, G.R., 1973. Cryogenic Insulation Heat Transfer. *Advances in Heat Transfer 9*, 349-417. Elsevier. doi:10.1016/S0065-2717(08)70065-0.